2005-06

"Follow the leader" formation control of multiple autonomous underwater vehicles using forward looking sonar

Grabelle, Jason

Monterey, California. Naval Postgraduate School

NAVAL POSTGRADUATE SCHOOL

MONTEREY, CALIFORNIA

THESIS

"FOLLOW THE LEADER": FORMATION CONTROL OF MULTIPLE AUTONOMOUS UNDERWATER VEHICLES USING FORWARD LOOKING SONAR

by

Jason Grabelle

June 2005

Thesis Advisor: Anthony J. Healey

Approved for public release; distribution is unlimited

THIS PAGE INTENTIONALLY LEFT BLANK

REPORT DOCUMENTATION PAGE			Form Approved OMB No. 0704-0188
Public reporting burden for this collection of information is estimated to average 1 hour per response, including the time for reviewing instruction, searching existing data sources, gathering and maintaining the data needed, and completing and reviewing the collection of information. Send comments regarding this burden estimate or any other aspect of this collection of information, including suggestions for reducing this burden, to Washington headquarters Services, Directorate for Information Operations and Reports, 1215 Jefferson Davis Highway, Suite 1204, Arlington, VA 22202-4302, and to the Office of Management and Budget, Paperwork Reduction Project (0704-0188) Washington DC 20503.			
1. AGENCY USE ONLY *(Leave blank)*	**2. REPORT DATE** June 2005	**3. REPORT TYPE AND DATES COVERED** Master's Thesis	
4. TITLE AND SUBTITLE: "Follow the Leader": Formation Control of Multiple Autonomous Vehicles Using Forward Looking Sonar			**5. FUNDING NUMBERS**
6. AUTHOR: Grabelle, Jason			
7. PERFORMING ORGANIZATION NAME(S) AND ADDRESS(ES) Naval Postgraduate School Monterey, CA 93943-5000			**8. PERFORMING ORGANIZATION REPORT NUMBER**
9. SPONSORING /MONITORING AGENCY NAME(S) AND ADDRESS(ES) N/A			**10. SPONSORING/MONITORING AGENCY REPORT NUMBER**
11. SUPPLEMENTARY NOTES The views expressed in this thesis are those of the author and do not reflect the official policy or position of the Department of Defense or the U.S. Government.			
12a. DISTRIBUTION / AVAILABILITY STATEMENT Approved for public release; distribution is unlimited			**12b. DISTRIBUTION CODE**

13. ABSTRACT (maximum 200 words)

With the Global War on Terrorism (GWOT) taking place in full force, autonomous vehicles have become a major asset to government forces. Expansion of single vehicle technology to multiple vehicle technology is required in order for the United States to stay ahead of its adversaries in the GWOT and other technological fields (such as oceanography). Multiple vehicle technology has been explored by many different institutions in the recent past (Leonard, 2001 and Kucik, 2003). Expansion of this technology will lead to greater autonomy and robustness amongst the vehicles. This thesis presents a simulation of a "follow the leader" behavior for multiple Autonomous Underwater Vehicles (AUVs). The follower vehicle incorporates the use of forward-looking sonar to track the leader vehicle. This process will free up bandwidth between acoustic modems; allowing data transfer to occur with greater efficiency. Hydrodynamic coefficients are used to develop steering equations that model REMUS through a track of specified waypoints similar to a real-world mission track. A two-dimensional forward looking sonar model with a 120^{o} horizontal scan and a 110 meter radial range is modeled to track the leader vehicle. Resulting bearing and range between the two vehicles is incorporated as control for positioning the follower vehicle.

14. SUBJECT TERMS Formation, Underwater vehicle, AUV, REMUS, Follow the leader			**15. NUMBER OF PAGES** 59
			16. PRICE CODE
17. SECURITY CLASSIFICATION OF REPORT Unclassified	**18. SECURITY CLASSIFICATION OF THIS PAGE** Unclassified	**19. SECURITY CLASSIFICATION OF ABSTRACT** Unclassified	**20. LIMITATION OF ABSTRACT** UL

NSN 7540-01-280-5500 Standard Form 298 (Rev. 2-89)
Prescribed by ANSI Std. 239-18

THIS PAGE INTENTIONALLY LEFT BLANK

Approved for public release; distribution is unlimited

"FOLLOW THE LEADER": FORMATION CONTROL OF MULTIPLE AUTONOMOUS UNDERWATER VEHICLES USING FORWARD LOOKING SONAR

Jason Grabelle
Lieutenant, United States Navy
B.S., Maine Maritime Academy, 1998

Submitted in partial fulfillment of the
requirements for the degree of

MASTER OF SCIENCE IN MECHANICAL ENGINEERING

from the

NAVAL POSTGRADUATE SCHOOL
June 2005

Author: Jason Grabelle

Approved by: Anthony J. Healey
Thesis Advisor

Anthony J. Healey
Chairman, Department of Mechanical and
Astronautical Engineering

THIS PAGE INTENTIONALLY LEFT BLANK

ABSTRACT

With the Global War on Terrorism (GWOT) taking place in full force, autonomous vehicles have become a major asset to government forces. Expansion of single vehicle technology to multiple vehicle technology is required in order for the United States to stay ahead of its adversaries in the GWOT and other technological fields (such as oceanography). Multiple vehicle technology has been explored by many different institutions in the recent past (Leonard, 2001 and Kucik, 2003). Expansion of this technology will lead to greater autonomy and robustness amongst the vehicles. This thesis presents a simulation of a "follow the leader" behavior for multiple Autonomous Underwater Vehicles (AUVs). The follower vehicle incorporates the use of forward-looking sonar to track the leader vehicle. This process will free up bandwidth between acoustic modems; allowing data transfer to occur with greater efficiency. Hydrodynamic coefficients are used to develop steering equations that model REMUS through a track of specified waypoints similar to a real-world mission track. A two-dimensional forward looking sonar model with a 120^{o} horizontal scan and a 110 meter radial range is modeled to track the leader vehicle. Resulting bearing and range between the two vehicles is incorporated as control for positioning the follower vehicle.

THIS PAGE INTENTIONALLY LEFT BLANK

TABLE OF CONTENTS

THIS PAGE INTENTIONALLY LEFT BLANK

LIST OF FIGURES

THIS PAGE INTENTIONALLY LEFT BLANK

LIST OF TABLES

THIS PAGE INTENTIONALLY LEFT BLANK

ACKNOWLEDGMENTS

I would like to thank my thesis advisor, Professor Anthony Healey, for his expert insight, direction, and assistance during the development of this work. Not only did he teach me in the classroom and in the field but through his example as a dedicated professional.

I would like to thank my family. To my wonderful wife, Deanna, I want you to know how much I appreciate the support and encouragement you always provide. To my children, Logan and Wyatt, I thank you for your patience and understanding when I could not always be there for you.

THIS PAGE INTENTIONALLY LEFT BLANK

I. INTRODUCTION

A. BACKGROUND

An Autonomous Underwater Vehicle (AUV) is an unmanned, self-propelled vehicle that is able to provide data storage as well as make navigational and tactical decisions based on inputs from onboard sensors. Typically, data collected from inertial sensors is integrated and processed by an onboard computer in order to estimate the position and orientation of the vehicle. This onboard computer also controls the vehicle; allowing it to complete its mission with very little human interaction. AUV's are typically battery powered. However, many different power sources have been experimented with recently in order to meet the needs of increased mission length (Miller, 2002). Development of AUV's began as far back as 1960. For a history on AUV development, see (Blidberg, 2001). AUV's are developed by many different institutions; to include government, commercial, and educational.

Today, with the Global War on Terrorism currently taking place, the United States Navy employs a wide range of AUV's to meet the ever expanding requirements set forth by current and future strategy. In recent years, the United States Navy has adopted a strategy that shifts its priorities from blue water to littoral operations and amphibious support. Sea Power 21, the current Navy strategy, directs the "use of unmanned platforms: Air, Land, Sea, and Undersea for combat and reconnaissance (Clarke, 2002)." The Navy has determined that there are nine key mission areas that Unmanned Underwater Vehicles (UUV's) must be designed for in order to be successful in today's battle arena as well as the battle arena 50 years from now. These mission areas include: 1) intelligence, surveillance, and reconnaissance; 2) mine countermeasures; 3) anti-submarine warfare; 4) inspection/identification; 5) oceanography; 6) communication/navigation network node; 7) payload delivery; 8) information operations; and 9) time critical strikes (UUV Master Plan, 2004).

B. MOTIVATION

The primary motivating factor behind this research is to allow formation flying of AUV's to occur without the use of an acoustic modem as the primary source of communicating position between the vehicles. This will free up bandwidth exchanged between acoustic modems located on each vehicle. This additional bandwidth will allow for an increased efficiency in the transfer of mission data between vehicles; which in turn will allow for operators to receive data quicker (helping with planning and executing of real world missions).

A secondary motivating factor behind this research is to give vehicles the capability to become more robust and autonomous. The addition of forward looking sonar to the Remote Environmental Measuring Unit System (REMUS) vehicle will allow this to occur. In addition to multiple vehicle control, forward looking sonar will allow for obstacle avoidance (Fodrea, 2002). This thesis will present a solution to the formation flying problem for multiple AUV's.

C. FORMATION FLYING FOR AUTONOMOUS UNDERWATER VEHICLES

In order to stay ahead of its adversaries, the United States must switch from single AUV technology to multi-AUV technology. This switch in design and mission planning has been examined by many different institutions in recent years. Early research in this area had vehicles relying on beacons or locator sensors in order to control the formation. More recently, "follow the leader" behaviors have been designed to rely on ranging and intention information shared between vehicles using acoustic communications (Kucik, 2003). This thesis will go one step further and concentrate on using a "follow the leader" behavior that relies on ranging and bearing information received from forward looking sonar.

D. THE REMUS VEHICLE

The original REMUS vehicle was developed at Wood's Hole Oceanographic Institute (WHOI). In 2001, REMUS entered commercial production and is now sold by

Hydroid, Inc. REMUS is used for a number of applications including harbor security and mine countermeasure operations.

It is designed to perform in the Very Shallow Water (VSW) zone from 40 to 100 feet. As seen in Figure 1, it is a two-man portable system that is 7.5" (19 cm) in diameter, 63" (160 cm) long, and weighs 80 pounds (37 kg). REMUS can reach a maximum speed of 5.45 knots (2.8 m/s) and a maximum depth 328 feet (100 m). Table 1 includes functional and physical specifications of the REMUS vehicle.

Figure 1. REMUS Vehicle (from Hydroid Inc., 2005)

REMUS can be configured with many different types of sensors, such as: side scan sonar, an acoustic doppler current profiler (ADCP), inertial navigation system, and acoustic modem. The navigation system includes a compass, the above-mentioned ADCP to provide speed over ground when ground lock is available, and an acoustic long-baseline (LBL) system to correct accumulated dead reckoning errors. Currently side-scan sonars are used to detect object on or near the sea floor. However, the addition of forward-looking sonar would give it the ability to detect objects (such as another AUV or uncharted sea mounts) in front of the vehicle.

PHYSICAL/FUNCTIONAL AREA	CHARACTERISTIC
Vehicle Diameter	19 cm
Vehicle Length	160 cm
Weight in Air	37 kg (<80 lbs.)
Trim Weight in Air	1 kg
Maximum Operating Depth	100 meters
Energy	1kw-hr internally rechargeable Lithium ion
Endurance	22 hours at optimum speed of 1.5m/s (3 knots). 8 hours at 2.5m/s (5 knots)
Propulsion	Direct dive DC brushless motor to open three bladed propeller
Velocity Range	0.25 to 2.8 m/s variable over range
Control	2 coupled yaw and pitch fins
On/Off	Magnetic switch
External Hook-up	Two pin combined Ethernet, vehicle power and battery charging; 4pin serial connector
Navigation	Long base line; Ultra short base line; Doppler assisted dead reckon; (Optional: GPS)
Transponders	20-30 kHz operating frequency range
Tracking	Emergency transponder, mission abort, and ORE Trackpoint compatible
Sensors Doppler Velocity Log	RDI 1.2 MHz up/down looking
Side Scan Sonar	600 or 900 kHz MSTL AUV model

Table 1. REMUS Specifications (from Hydroid Inc., 2005)

E. THESIS STRUCTURE

The intent of this research is to develop a forward looking sonar model that supports "follow the leader" behaviors of multiple REMUS vehicles. This is a two step process accomplished through the following: firstly, develop a robust steering model of two independently controlled REMUS vehicles and have them navigate a set of waypoints; secondly, adapt the steering model so that the second vehicle steering is dependent and controlled by the first vehicle's steering model.

Chapter II will focus on the development of the equations of motion for the REMUS AUV. Chapter III explains the theory and equations used for triangulating positions using ranging information.

Chapter IV describes the steering control laws associated with the EOM for REMUS. Chapter V will present a simulation for the "follow the leader" behavior using forward looking sonar. Chapter VI provides thesis conclusions and recommendations for future work.

THIS PAGE INTENTIONALLY LEFT BLANK

II. STEERING MODEL

A. GENERAL

Rigid body models are formed in order to analyze, predict, and control motion behavior of autonomous machines that travel over land, air, and undersea. Each type of vehicle model differs in only the terms of the forces applied to produce motion. However, these forces are often controllable and can thus be studied from a prospective of stabilization. This chapter will only deal with the modeling of underwater vehicles. The approach taken with underwater vehicles is that of a moving body in free space without constraint. The forces applied to underwater vehicles include the following: inertial, gravitational, hydrostatic, propulsion, thruster, and hydrodynamic lift and drag forces. (Healey class notes).

B. EQUATIONS OF MOTION IN THE HORIZONTAL PLANE

The following paragraphs describe a simplified development of the steering model used to control the REMUS vehicle. For a more detailed development, see (Healey, 1995). This model was adapted from that of the ARIES AUV (Healey and Marco, 2001) and is based on the following assumptions:

- the vehicle behaves as a rigid body
- the earth's rotation is negligible for acceleration components of the vehicle's center of mass
- the primary forces that act on the vehicle are inertial and gravitational in origin and are derived from hydrostatic, propulsion, thruster, and hydrodynamic lift and drag forces.

Before describing the equations of motion (EOM) that govern the REMUS steering model, a coordinate system for the vehicle and its surrounding area must be defined. The EOM are derived using a Newton-Euler approach that relates the position and motions in the local plane to those in the global plane. The geometry of the local and global coordinate system can be seen in Figure 2.

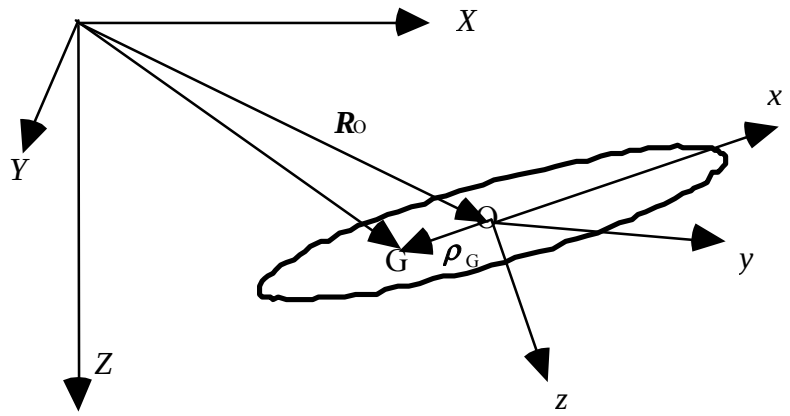

Figure 2. Local and Global Coordinate System (from Marco and Healey, 2001)

In order to convert from a local velocity vector $[u, v, w]$, where u is surge, v is sway, and w is heave, to a global velocity vector $[\dot{X}, \dot{Y}, \dot{Z}]$, a transformation matrix containing 'Euler' angles (ϕ, θ, ψ) must be defined. The transformation matrix (T) is defined as follows:

$$\mathbf{T}(\phi,\theta,\psi) = \begin{bmatrix} \cos\psi\cos\theta, & \sin\psi\cos\theta, & -\sin\theta \\ \cos\psi\sin\theta\sin\phi - \sin\psi\cos\phi, & \sin\psi\sin\theta\sin\phi + \cos\psi\cos\phi, & \cos\theta\sin\phi \\ \cos\psi\sin\theta\cos\phi + \sin\psi\sin\phi, & \sin\psi\sin\theta\cos\phi - \cos\psi\sin\phi, & \cos\theta\cos\phi \end{bmatrix} \quad (1)$$

Transformation from a global velocity vector to the local velocity vector occurs as follows:

$$\begin{bmatrix} u \\ v \\ w \end{bmatrix} = \mathbf{T}(\phi,\theta,\psi) \bullet \begin{bmatrix} \dot{X} \\ \dot{Y} \\ \dot{Z} \end{bmatrix} \quad (2)$$

Transformation from a local velocity vector to a global velocity vector occurs as follows:

$$\begin{bmatrix} \dot{X} \\ \dot{Y} \\ \dot{Z} \end{bmatrix} = \mathbf{T}^{-1}(\phi,\theta,\psi) \bullet \begin{bmatrix} u \\ v \\ w \end{bmatrix} \quad (3)$$

The global angular velocity vector $[p,q,r]$ can be transformed into the rates of change of the 'Euler' angles as follows:

$$\begin{bmatrix}\dot{\phi}\\ \dot{\theta}\\ \dot{\psi}\end{bmatrix}=\begin{bmatrix}1 & \sin\phi\tan\theta & \cos\phi\tan\theta\\ 0 & \cos\phi & -\sin\phi\\ 0 & \sin\phi/\cos\theta & \cos\phi/\cos\theta\end{bmatrix}\begin{bmatrix}p\\ q\\ r\end{bmatrix} \tag{4}$$

Healey (1995) derives the equations of motion for a six degree model as:

SURGE EQUATION OF MOTION

$$m\left[\dot{u}_r - v_r r + w_r q - x_G\left(q^2+r^2\right)+y_G\left(pq-\dot{r}\right)+z_G\left(pr+\dot{q}\right)\right]+\left(W-B\right)\sin\theta = X_f \tag{5}$$

SWAY EQUATION OF MOTION

$$m\left[\dot{v}_r + u_r r - w_r p + x_G\left(pq+\dot{r}\right)-y_G\left(p^2+r^2\right)+z_G\left(qr-\dot{p}\right)\right]-\left(W-B\right)\cos\theta\sin\phi = Y_f \tag{6}$$

HEAVE EQUATION OF MOTION

$$m\left[\dot{w}_r - u_r q + v_r p + x_G\left(pr-\dot{q}\right)+y_G\left(qr+\dot{p}\right)-z_G\left(p^2+q^2\right)\right]+\left(W-B\right)\cos\theta\cos\phi = Z_f \tag{7}$$

ROLL EQUATION OF MOTION

$$I_x\dot{p}+\left(I_z-I_y\right)qr+I_{xy}\left(pr-\dot{q}\right)-I_{yz}\left(q^2-r^2\right)-I_{xz}\left(pq+\dot{r}\right)+m\left[y_G\left(\dot{w}-u_r q+v_r p\right)\right. \tag{8}$$

$$\left.-z_G\left(\dot{v}_r+u_r r-w_r p\right)\right]-\left(y_G W-y_B B\right)\cos\theta\cos\phi+\left(z_G W-z_B B\right)\cos\theta\sin\phi = K_f \tag{9}$$

PITCH EQUATION OF MOTION

$$I_y\dot{q}+\left(I_z-I_z\right)pr-I_{xy}\left(qr+\dot{p}\right)+I_{yz}\left(pq-\dot{r}\right)+I_{xz}\left(p^2-r^2\right)-m\left[x_G\left(\dot{w}-u_r q+v_r p\right)\right. \tag{10}$$

$$\left.-z_G\left(\dot{u}_r-v_r r+w_r q\right)\right]+\left(x_G W-x_B B\right)\cos\theta\cos\phi+\left(z_G W-z_B B\right)\sin\theta = M_f$$

YAW EQUATION OF MOTION

$$I_z\dot{r}+\left(I_y-I_x\right)pq-I_{xy}\left(p^2-q^2\right)-I_{yz}\left(pr+\dot{q}\right)+I_{xz}\left(qr-\dot{p}\right)+m\left[x_G\left(\dot{v}_r+u_r r-w_r p\right)\right. \tag{11}$$

$$\left.-y_G\left(\dot{u}_r-v_r r+w_r q\right)\right]-\left(x_G W-x_B B\right)\cos\theta\sin\phi-\left(y_G W-y_B B\right)\sin\theta = N_f$$

Where:

W = weight
B = buoyancy
I = mass moment of inertia terms
u_r, v_r, w_r = component velocities for a body fixed system with respect to the water
p, q, r = component angular velocities for a body fixed system
x_B, y_B, z_B = position difference between geometric center and center of buoyancy
x_G, y_G, z_G = position difference between geometric center and center of gravity
X_f, Y_f, Z_f, K_F, M_f, N_f = sums of all external forces acting in the particular body fixed direction

In addition, he presents a simplified version of these equations of motion. In order to simplify the initial equations of motions the following assumptions were made:

- the center of mass of the vehicle lies below the origin
- x_g and y_g are zero
- the vehicle is symmetric in its inertial properties
- motions in the vertical plane are negligible (i.e., [w_r, p, q, r, Z, ϕ, θ]=0)
- u_r equals the forward speed, U_o

The simplified equations of motion are thus:

$$u_r = U_o \tag{12}$$

$$m\dot{v}_r = -mU_o r + \Delta Y_f(t) \tag{13}$$

$$I_{zz}\dot{r} = \Delta N_f(t) \tag{14}$$

$$\dot{\psi} = r \tag{15}$$

$$\dot{X} = U_o \cos\psi - v_r \sin\psi + U_{cx} \tag{16}$$

$$\dot{Y} = U_o \sin\psi - v_r \cos\psi + U_{cy} \tag{17}$$

C. HYDRODYNAMIC COEFFICIENTS

Healey proposes that due to symmetry of the vehicle, one can heuristically determine that only a subset of motions would affect the loading in any particular direction (Healey class notes) and uses the following expressions to describe hydrodynamic forces of sway and yaw:

$$\Delta Y_f = f(v_r, dv_r/dt, r, dr/dt, p, dp/dt, t) \tag{18}$$

$$\Delta N_f = f(p, dp/dt, v_r, dv_r/dt, r, dr/dt, t) \tag{19}$$

Sway, yaw, and roll motions are coupled. However, roll motion is often only coupled one way and not considered when evaluating horizontal plane steering. The hydrodynamic forces for sway and yaw are linearized using Taylor series expansion to determine 'hydrodynamic coefficients.' The coefficients are dependent on the shape characteristics of the vehicle and have significant affect on the natural stability of the vehicle. The expression for the transverse (sway) force is:

$$Y_f = Y_{\dot{v}_r}\dot{v}_r + Y_{v_r}v_r + Y_{\dot{r}}\dot{r} + Y_r r \tag{20}$$

and the expression for rotational (yaw) force is:

$$N_f = N_{\dot{v}_r}\dot{v}_r + N_{v_r}v_r + N_{\dot{r}}\dot{r} + N_r r \tag{21}$$

This leads to:

$$Y_{v_r} = \frac{\partial Y_f}{\partial v_r};\ \ \mathrm{Y}_r = \frac{\partial N_f}{\partial r};\ \ \mathrm{Y}_{\dot{v}_r} = \frac{\partial Y_f}{\partial \dot{v}_r};\ \ \mathrm{Y}_{\dot{r}} = \frac{\partial Y_f}{\partial \dot{r}}; \tag{22}$$

and

$$N_{v_r} = \frac{\partial N_f}{\partial v_r};\ \ \mathrm{N}_r = \frac{\partial N_f}{\partial r};\ \ \mathrm{N}_{\dot{v}_r} = \frac{\partial N_f}{\partial \dot{v}_r};\ \ \mathrm{N}_{\dot{r}} = \frac{\partial N_f}{\partial \dot{r}}; \tag{23}$$

Where:

$Y_{\dot{v}_r}$ = coefficient for added mass in sway

$Y_{\dot{r}}$ = coefficient for added mass in yaw

Y_{v_r} = coefficient of sway force induced by side slip

Y_r = coefficient of sway force induced by yaw

$N_{\dot{v}_r}$ = coefficient for added mass moment of inertia in sway

$N_{\dot{r}}$ = coefficient for added mass moment of inertia in yaw

N_{v_r} = coefficient of sway moment from side slip

N_r = coefficient of sway moment from yaw

The hydrodynamic coefficients for steering for the REMUS vehicle were adapted from thesis work performed by MIT (Prestero, 2001) establishing estimates of all vehicle coefficients. Upon re-calculation, Fodrea (2002) adjusted the hydrodynamic coefficients to account for variation in experimental data. Table 2 lists the REMUS hydrodynamic coefficients for the steering model used during this experiment.

$Y_{\dot{v}_r}$	-3.55e01 kg
$Y_{\dot{r}}$	1.93 kg m/rad
Y_{v_r}	-6.66e01 kg/s (Same as Zw)
Y_r	2.2 kg m/s (Same as Zq)
$N_{\dot{v}_r}$	1.93 kg m
$N_{\dot{r}}$	-4.88 kg m^2/rad
N_{v_r}	-4.47 kg m/s
N_r	-6.87 kg m^2/s (Same as Mq)
N_d	-3.46e01/3.5 kg m/s^2
Y_d	5.06e01/3.5 kg m/s^2

Table 2. REMUS Hydrodynamic Coefficients for Steering (from Fodrea, 2002)

The dynamics of the vehicles are defined as:

$$m\dot{v}_r = -mr + Y_{\dot{v}_r}\dot{v}_r + Y_{v_r}v_r + Y_{\dot{r}}\dot{r} + Y_r r + Y_\delta \delta_r(t) \tag{25}$$

$$I_{zz}\dot{r} = N_{\dot{v}_r}\dot{v}_r + N_{v_r}v_r + N_{\dot{r}}\dot{r} + N_r r + N_\delta \delta_r(t) \tag{26}$$

$$\dot{\psi} = r \tag{27}$$

D. VEHICLE KINEMATICS

The kinematics of the vehicle is described by Equations (25) and (26). U_{cx} and U_{cy} are the current velocities in the associated direction. The kinematic equations, along with the heading rate, compose the steering dynamics of REMUS and can be expressed as follows:

$$\begin{bmatrix} m - Y_{\dot{v}_r} & -Y_{\dot{r}} & 0 \\ -N_{\dot{v}_r} & I_{zz} - N_{\dot{r}} & 0 \\ 0 & 0 & 1 \end{bmatrix} \begin{bmatrix} \dot{v}_r \\ \dot{r} \\ \dot{\psi} \end{bmatrix} = \begin{bmatrix} Y_{v_r} & Y_r - mU_0 & 0 \\ N_{v_r} & N_r & 0 \\ 0 & 0 & 1 \end{bmatrix} \begin{bmatrix} v_r \\ r \\ \psi \end{bmatrix} + \begin{bmatrix} Y_\delta \\ N_\delta \\ 0 \end{bmatrix} \delta_r(t) \tag{28}$$

where $\delta_r(t)$ represents the control input for both rudders.

E. VEHICLE DYNAMICS

The final assumption made for vehicle dynamics (Johnson, 2001) is that the cross coupling terms in the mass matrix is zero. Thus, the final vehicle dynamics are defined as:

$$\begin{bmatrix} m - Y_{\dot{v}_r} & 0 & 0 \\ 0 & I_{zz} - N_{\dot{r}} & 0 \\ 0 & 0 & 1 \end{bmatrix} \begin{bmatrix} \dot{v}_r \\ \dot{r} \\ \dot{\psi} \end{bmatrix} = \begin{bmatrix} Y_{v_r} & Y_r - mU_0 & 0 \\ N_{v_r} & N_r & 0 \\ 0 & 0 & 1 \end{bmatrix} \begin{bmatrix} v_r \\ r \\ \psi \end{bmatrix} + \begin{bmatrix} Y_\delta \\ N_\delta \\ 0 \end{bmatrix} \delta_r(t) \tag{29}$$

THIS PAGE INTENTIONALLY LEFT BLANK

III. TRIANGULATION THEORY: GEOMETRY AND EQUATIONS

A. INTRODUCTION

Triangulation is one of the most common methods for determining position. It is used on many different navigation systems including: Long Base Line (LBL), Global Positioning System (GPS), and LORAN. The simplest method of triangulation is where the vehicle's range from two known points is used to determine the vehicle's position. However, despite its simplicity, there are still some ambiguities associated with this process. Figure 3 shows how an LBL system is not able to determine where the vehicle is located because the range rings centered on the transponders intersect in two places.

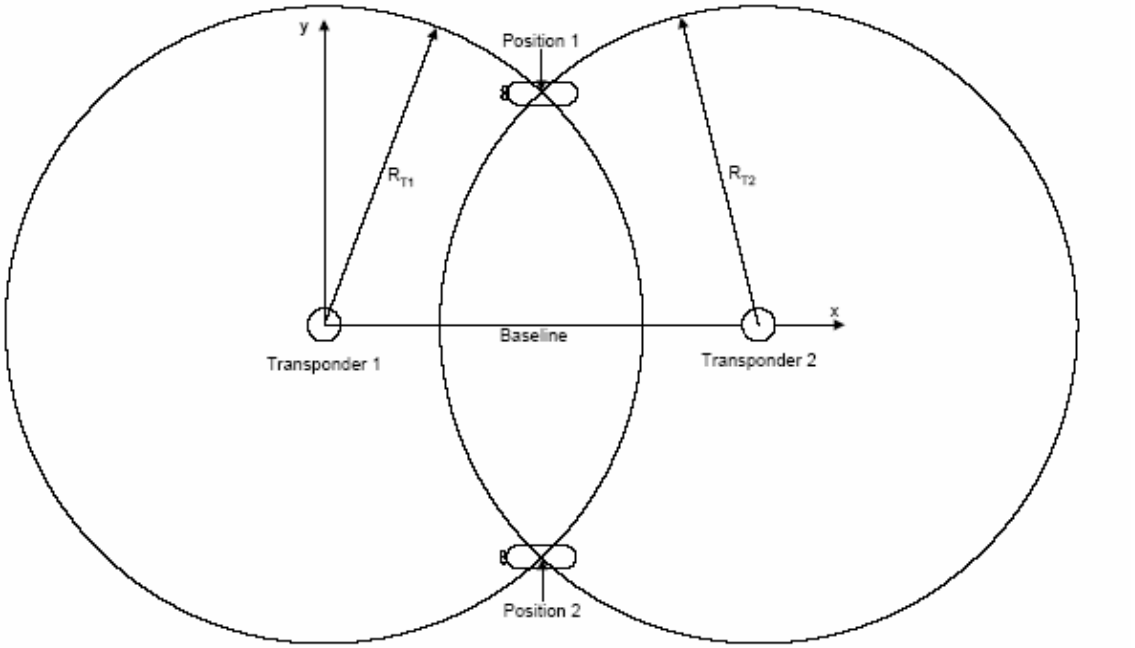

Figure 3. LBL System (from Kucik, 2003)

Throughout this thesis, it was assumed that the leader vehicle had an advanced navigation system (to include GPS) onboard and can accurately determine its position throughout the simulation.

B. TRIANGULATION GEOMETRY AND EQUATIONS

Triangulation geometry can be used to determine the range and bearing between the leader and follower vehicles based on their position. Figure 4 is a simplified triangulation computation using the x and y values of both vehicle's position.

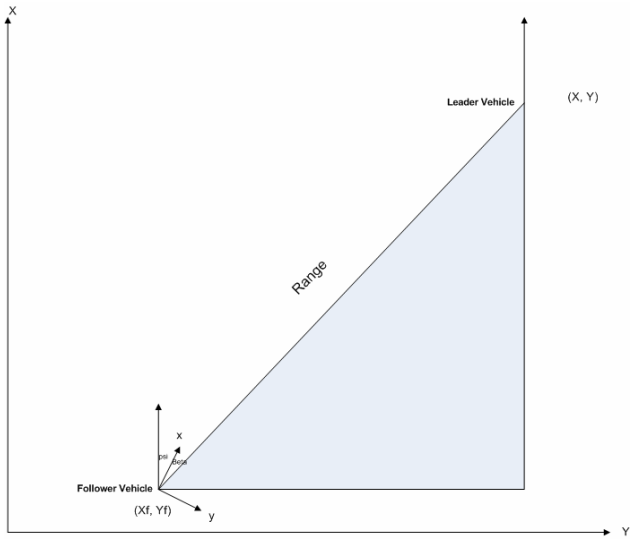

As seen in Figure 4, and based on the Law of Cosines, the following formulas are defined for range and bearing:

$$\text{range} = \sqrt{(Y - Y_f)^2 + (X - X_f)^2} \tag{30}$$

where

Y = the y-position of the leader vehicle

Y_f = the y-position of the follower vehicle

X = the x-position of the leader vehicle

X_f = the x-position of the follower vehicle

and

$$\text{bearing}=\text{atan2}((Y - Y_f),(X - X_f)) - \psi_f \tag{31}$$

where ψ_f = follower vehicle heading

IV. CONTROL METHODS AND ARCHITECTURE

A. GENERAL CONTROL THEORY

An underwater vehicle operates with six degrees of freedom and must respond to hydrostatic and hydrodynamic forces from an ever changing ocean environment. In addition to responding to environmental factors, underwater vehicles also must overcome the fact that actuator dynamics are small, power and control is limited to onboard capacity of the vehicle, and human intervention to correct faults is not possible during a mission (Fodrea, 2002). In spite of the above conditions, feedback control has been a suitable solution used to provide commands to actuators that control and stabilize the motion of underwater vehicles (Healey and Marco, 2001).

One of the main objectives of autonomous vehicles is that they must be robust. Robustness is obtained by using feedback of key motion variables as obtained by sensors that drive actuators (Healey class notes). This in turn acts an autopilot and maneuvers the vehicle as set during mission pre-planning. Marco describes four different autopilots for flight maneuvering control. These consist of independent diving, steering/heading, altitude above bottom, and cross-track error controllers. The four modes are decoupled and are based on sliding mode control (SMC) theory. Sliding mode controls can compensate for nonlinear systems (Healey, 1992). It is a robust method with a theory which allows n^{th} order systems to be effectively replaced by a (n-1) order system. Two tuning factors are used in this model to include *Eta_FlightHeading*, η, and *Phi_FlightHeading,* ϕ, as seen in Appendix A.

B. REMUS CONTROL ARCHITECTURE

The original REMUS steering model, used in this thesis for the leader vehicle, was developed by Fodrea (2002). Both the leader and follower vehicles are modeled in two dimensional space. Due to this fact, the steering controller is the only autopilot controller necessary for modeling the leader vehicle. The leader vehicle is a second order model that uses r and ψ as feedback.

In order to reach all of the desired waypoints, line-of-sight guidance is also implemented. The follower vehicle's steering controller is not as advanced as the leader vehicle. The follower vehicles position is maintained by control laws incorporating range and bearing to the leader vehicle that is received from forward looking sonar.

C. SLIDING MODE CONTROL

A multivariable sliding mode controller is used to provide an accurate steering model. A multivariable controller is used with predominantly linear systems as opposed to the SMC methods used for nonlinear systems (Healey, 1992). To create the SMC, the general form of the equations of motion is used:

$$x = A\dot{x} + Bu \tag{32}$$

where $\mathbf{x} \in \Re^{n*1}, \mathbf{A} \in \Re^{n*n}, \mathbf{B} \in \Re^{n*r}, \mathbf{u} \in \Re^{r*1}$, and u is the rudder angle. The goal of a sliding surface it do drive the state to a stable solution ($\sigma = 0,\ \sigma \in \mathbb{R}^{\rho*1}$). The sliding surface is defined as:

$$\sigma = s'\tilde{x};\ \ \tilde{x} = x - x_{com} \tag{33}$$

where s' is a vector of directions in the state error space. The elements of σ are the lengths of the projections of the state error vector. x_{com} is a variable created as a command signal to track. $\tilde{x}$ is the state error which is required to be driven to zero so the command state equals the actual state. By definition of the sliding mode controller, the system dynamics must exhibit stable sliding on the surface when $\sigma = 0$. Therefore, s' can be determined by observing that the closed loop dynamics are given by the poles of the closed loop matrix as,

$$(A - bk_2) = A_c,\ with\ k_2 = [s'B]^{-1}s'A \tag{34}$$

where k_2 is chosen by pole placement and $A_c s' = 0$ to achieve the condition $\sigma = 0$. The eigenvectors of the A_c matrix determine the linear state feedback gains for each state to define the sliding surface as follows:

$$\sigma(t) = s_2(r_{com} - r(t)) + s_3\psi_{LOS}(t) \tag{35}$$

The poles selected for the REMUS model of the leader vehicle were similar to those selected by Fodrea (2002) in here simulation. As seen in Appendix A, the poles are places at [-1.4 -1.45 0.0]. A pole must be placed at the origin in order to represent the single sliding constraint for the single input system. The remaining poles are in the open left hand plane; which is a requirement for stable dynamics. The gains obtained from this pole placement, using the MATLAB command "place", where [k1 k2 k3] = [0.769 -0.6 0.0] for $[v, r, \psi]$ respectively. Using the gains determined from pole placement and the sliding surface defined in Equation(34), the commanded rudder in the LOS controller for the leader vehicle becomes:

$$dr(t) = -k2 * r(t) * \eta * \tanh\left(\frac{\sigma(t)}{\phi}\right) \tag{36}$$

where η and ϕ are tuning factors equal to 0.5 and 0.1.

D. LINE OF SIGHT GUIDANCE

A Line of Sight (LOS) controller is used on the leader vehicle. The purpose behind its use it reduce the heading error to zero. Once again, this controller was developed for the REMUS vehicle by Fodrea (2002). It uses a follow-the-rabbit technique which is similar in nature to the transducer based dead-reckoning approach with which REMUS operates with in the real world. This controller directs the vehicle towards the current waypoint. It achieves this by determining the heading error, ψ_{LOS} which is defined as:

$$\tilde{\psi}(t)_{LOS} = \psi(t)_{track} - \psi(t) \tag{37}$$

where

$$\psi(t)_{track} = \arctan(\tilde{Y}(t)_{wpt(i)}, \tilde{X}(t)_{wpt(i)}) \tag{38}$$

Figure 3 is a graphical representation of how the REMUS vehicle model incorporates an additional dead reckoning on the track towards the next waypoint. The distance to this point is incorporated into the heading error as follows:

$$\tilde{\psi}(t)_{LOS} = \psi(t)_{track} - \psi(t) - \arctan\left(\frac{cte(t)}{rabbit}\right) \tag{39}$$

where rabbit is the look ahead point and cte is the cross track error.

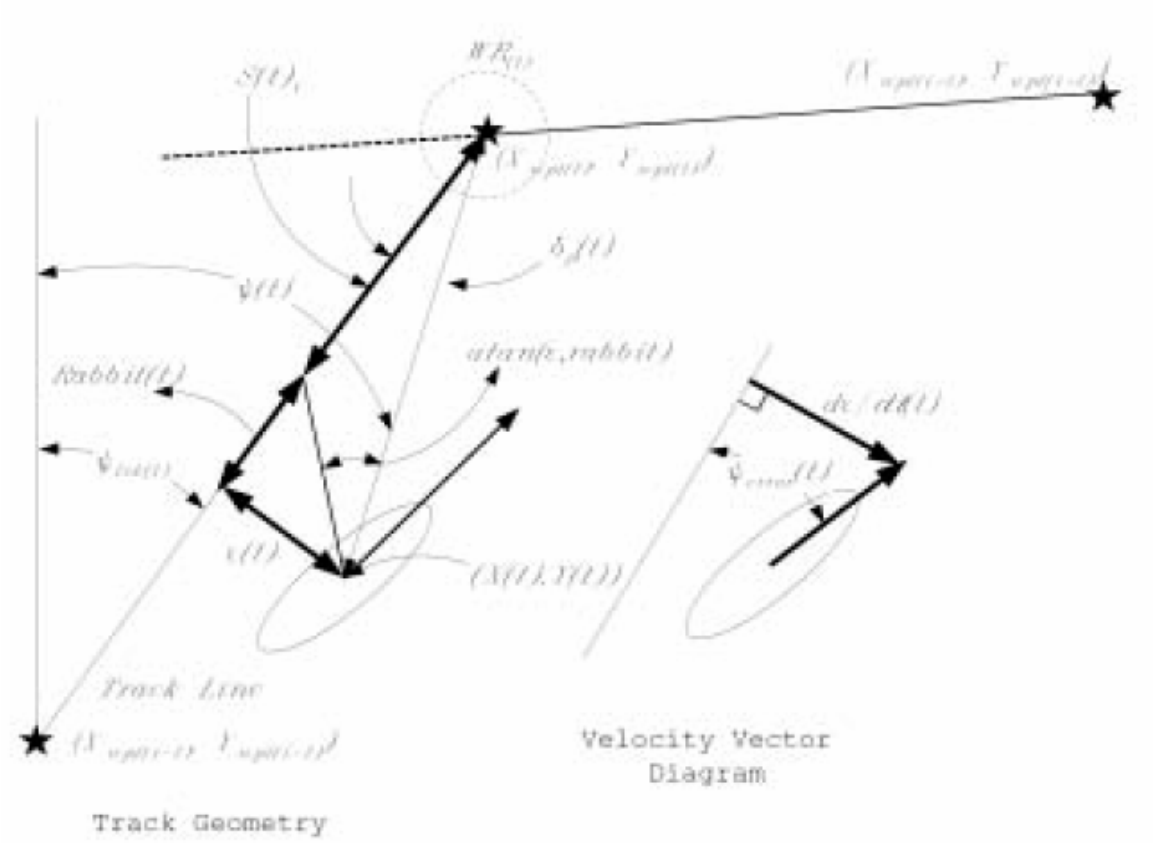

Figure 4. Track Geometry and Velocity Vector Diagram (from Fodrea, 2002)

As the leader vehicle approaches the waypoint, it must determine when to turn. In order to do this, REMUS will begin tracking the next waypoint when approaching the present waypoint based on the following formula:

$$sqrt(X\_Way\_Error(t)^2 + Y\_Way\_Error(t)^2 <= W\_R \left| S(t) < 0.0 \right| ss(t) < rabbit \tag{40}$$

where W_R is the watch radius around the waypoint, s is the distance remaining on the track, and ss is the radial distance to go to the next waypoint.

E. CONTROL LAWS FOR FOLLOWER VEHICLE

One of the primary objectives of this thesis was to design a set of control laws that would position the follower vehicle. As seen above with the leader vehicle, the control laws for the follower vehicle were designed based on sliding mode control. Control laws for the follower vehicle were based on incorporating range and bearing to the leader vehicle that was received from forward looking sonar.

Based on the range between the leader and the follower vehicle, the follower vehicle would adjust its speed (U) in order to achieve the command range (R_{com}). Range error is defined as:

$$\tilde{R} = (R(t) - R_{com}) \tag{41}$$

In order to determine the speed of the follower vehicle, the following formulas are defined:

$$\dot{\sigma}_R = -\eta \,\mathrm{sgn}(\sigma_R) \tag{42}$$

where $\sigma_R = \tilde{R}$. Also,

$$\dot{\sigma}_R = \dot{\tilde{R}} = (\dot{R} - 0) \tag{43}$$

$\dot{R}$ is defined as:

$$\dot{R} = \left(\frac{x_o - x}{R}\right)(\dot{x}_o - \dot{x}) + \left(\frac{y_o - y}{R}\right)(\dot{y}_o - \dot{y}) \tag{44}$$

where

$x_o =$ leader vehicle's x-position

$x =$ follower vehicle's x-position

$\dot{x}_o = U_o \cos(\psi_o)$

$\dot{x} = U \cos(\psi)$

$y_o =$ leader vehicle's y-position

$y =$ follower vehicle's y-position

$\dot{y}_o = U_o \sin(\psi_o)$

$\dot{y} = U \sin(\psi)$

Combining Equations (42) and (44) and solving for U results in the following formula:

$$U = \frac{-\text{sgn}(\tilde{R})R + \dot{x}_0(x - x_0) + \dot{y}_o(y - y_o)}{\cos\psi(x - x_0) + \sin\psi(y - y_o)} \tag{45}$$

Based on the bearing between the leader and the follower vehicle, the follower vehicle would adjust its heading (ψ_f) in order to achieve the command bearing (β_{com}). Bearing error is defined as:

$$\tilde{\beta} = (\beta(t) - \beta_{com}) \tag{46}$$

In order to determine the heading of the follower vehicle the following formulas are defined:

$$\dot{\sigma}_\beta = -\eta \,\text{sgn}(\tilde{\beta} + \lambda\dot{\tilde{\beta}}) \tag{47}$$

$$\delta_r = -\eta \,\text{sgn}(\tilde{\beta} + \lambda r) \tag{48}$$

After a trial and error period, the following formula was produced in order to provide stable results.

$$\delta_r = -5 * \tilde{\beta} + 10 * r \tag{49}$$

The formulas listed throughout this chapter are incorporated into the model as seen in Appendix A. Results based on these formulas are discussed later in this thesis (Chapter V).

V. VEHICLE SIMULATION

A. INTRODUCTION

A MATLAB script file (Appendix A) was written in order to simulate multi-vehicle operations. This script file contains control laws and cooperative behaviors that support and evaluate the "follow the leader" behavior presented in Chapter IV. The following settings were incorporated into the simulation:

- The minimum distance between the leader vehicle and the follower vehicle (Rcom) was set to 10 meters.
- The leader's vehicle speed is set to 1.543 m/s.
- The follower's minimum and maximum speed is set to 1 m/s and 2 m/s, respectively.

B. REMUS SEARCH PATH

Due to the autonomy of the vehicle, REMUS is pre-programmed with a planned path of travel before the mission begins. The search path is commonly referred to as the lawnmower technique and is used to cover a square grid area. This thesis models a REMUS path the uses rows approximately 150 meters in length with 100 meters of separation as seen in Figure 5.

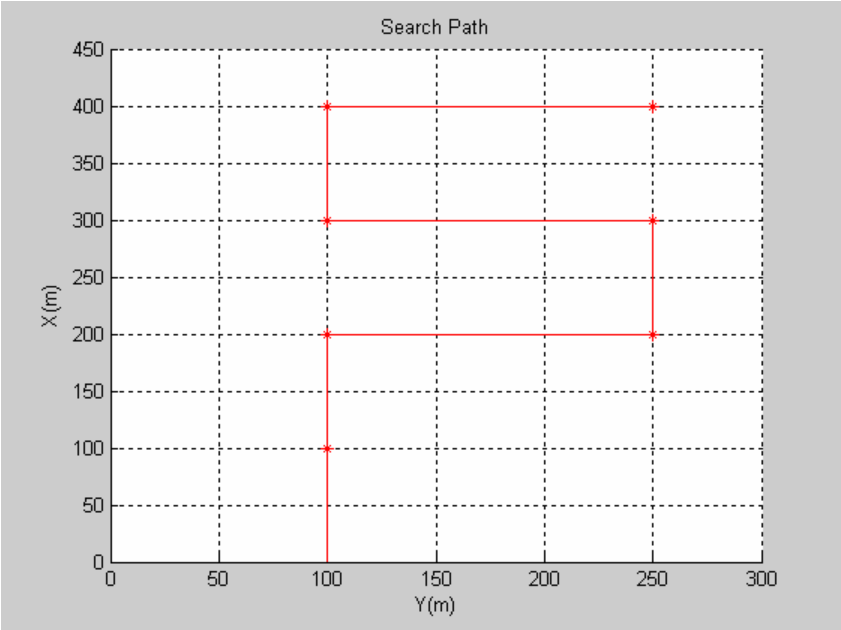

Figure 5. Typical REMUS Search Path

C. SONAR MODEL

This model uses a two dimensional forward looking sonar with a 120^{o} horizontal scan and a 110 meter radial range as seen in Figure 6. This is an estimated range based on a viable 400KHz sonar frequency. The use of forward looking sonar would alleviate exchanging position information via acoustic modem. Resulting bearing and range is used to control position of the follower vehicle.

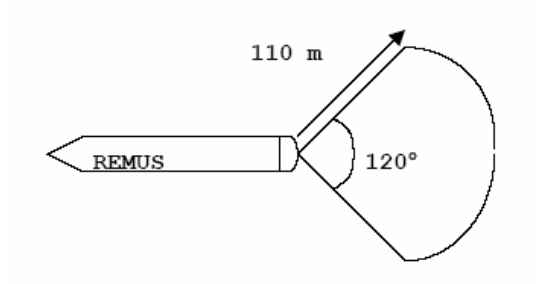

Figure 6. Forward Looking Sonar Model (from Fodrea, 2002)

D. MULTIPLE VEHICLE SIMULATION (NO CURRENT)

The first objective of this simulation was to have the leader and follower vehicle navigate a set of 7 waypoints depicting a typical "real world" search path. At this point, current was not injected into the simulation model. Figure 7 depicts the tracks for the leader and follower vehicles during the mission simulation.

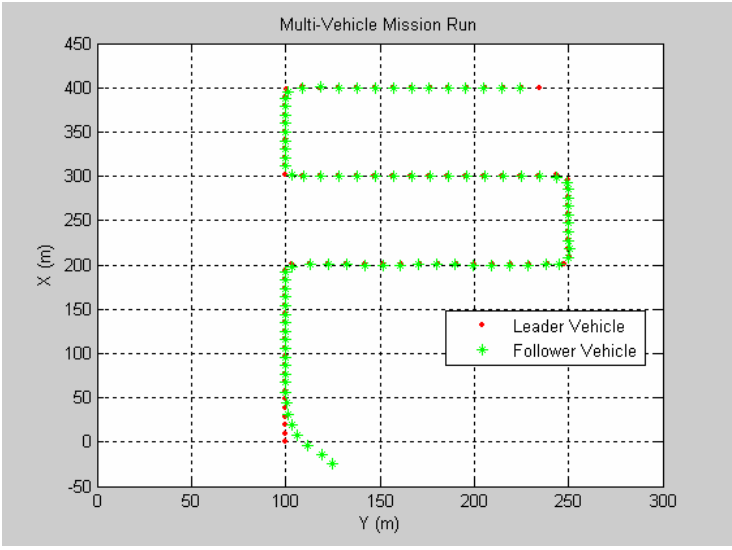

Figure 7. Leader and Follower Vehicle Path

Figure 8 shows an initial offset of the follower vehicle. This offset was performed in order to show the initial rendezvous between the leader and follower vehicles.

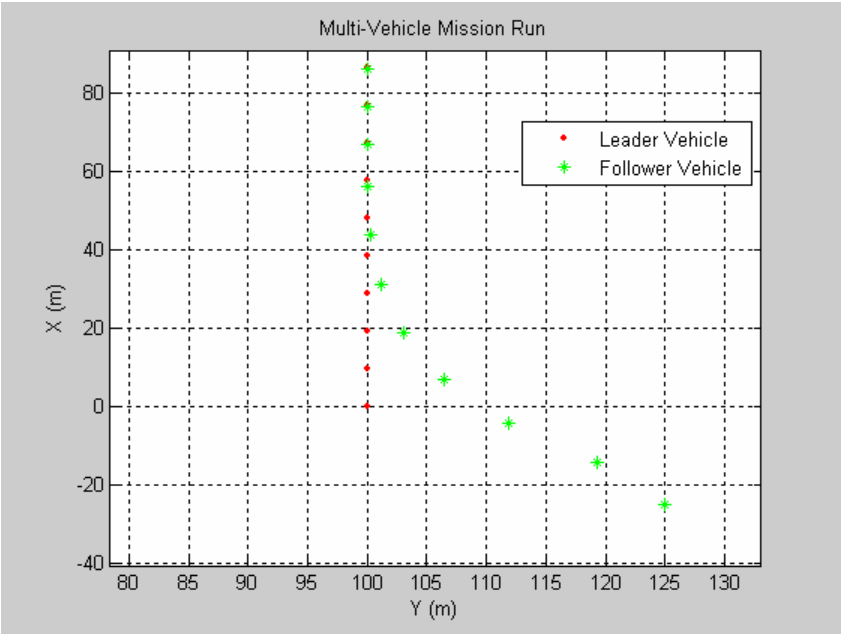

Figure 8. Initial Rendezvous Between Vehicles

Figures 9 and 10 show the range and bearing between the leader and the follower vehicle. Range and Bearing were the main variables in controlling the position of the follower vehicle. The command range was set to 10 meters and the command bearing was set to 0 degrees for this simulation.

From Figure 9, it is seen that initial range is approximately 35 meters. This is due to the initial offset. The range then decreases down to 10 meters as expected. Also, the range drops below 10 meters at 5 different locations during the simulation. This drop in range corresponds to the leader vehicle turning to the next waypoint.

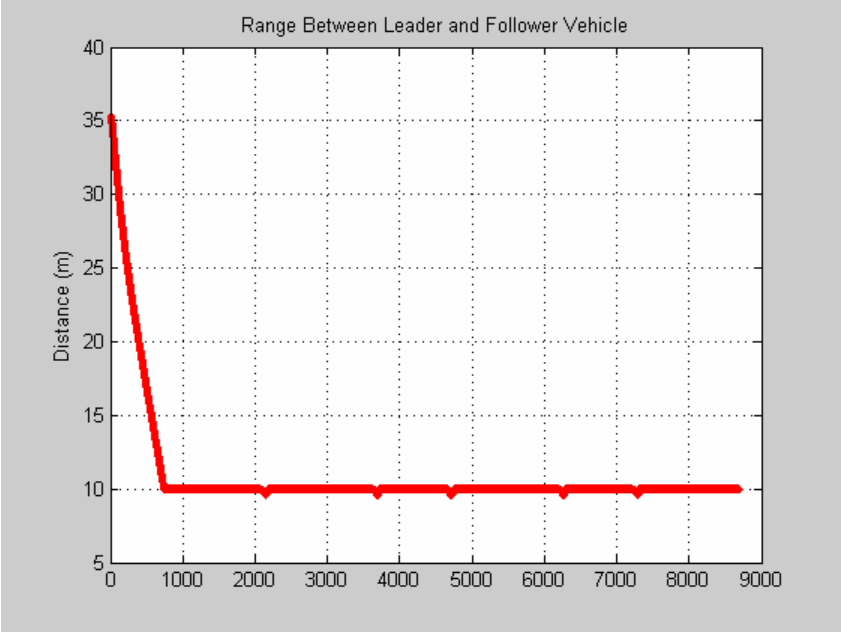

Figure 9. Range Between Leader and Follower Vehicle

From Figure 10, it is seen that initial bearing is approximately -45 degrees. As stated above, this is due to the initial offset of the follower vehicle. The bearing then decreases down to 0 degrees as expected. Bearing between the two vehicles changes during the turns as did the range

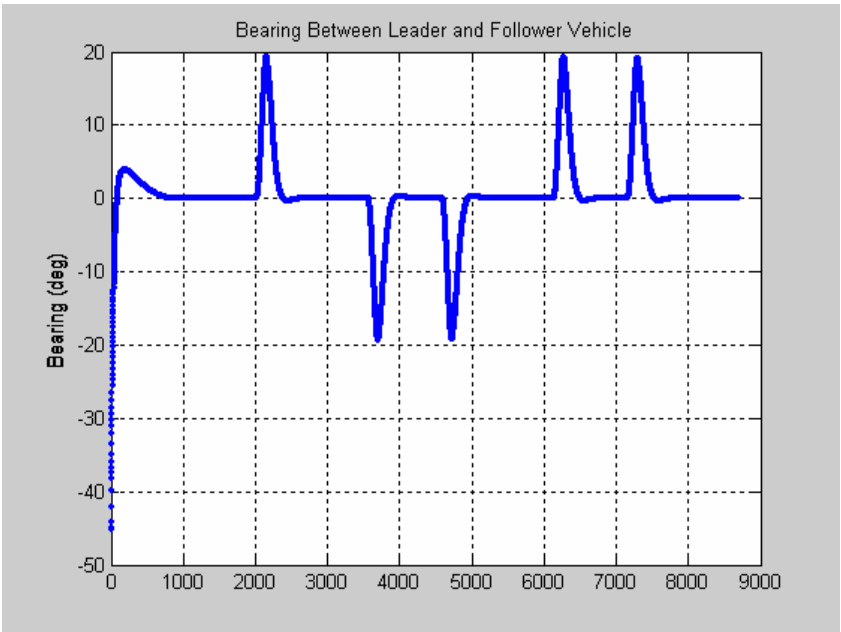

Figure 10. Bearing Between Leader and Follower Vehicle

Figures 11 and 12 contain a "zoomed in" look at the mission simulation. Specifically, Figure 11 is a "zoomed in" look at the vehicles while they are traveling in a straight line. Figure 12 is a "zoomed in" look at the vehicles during a turn.

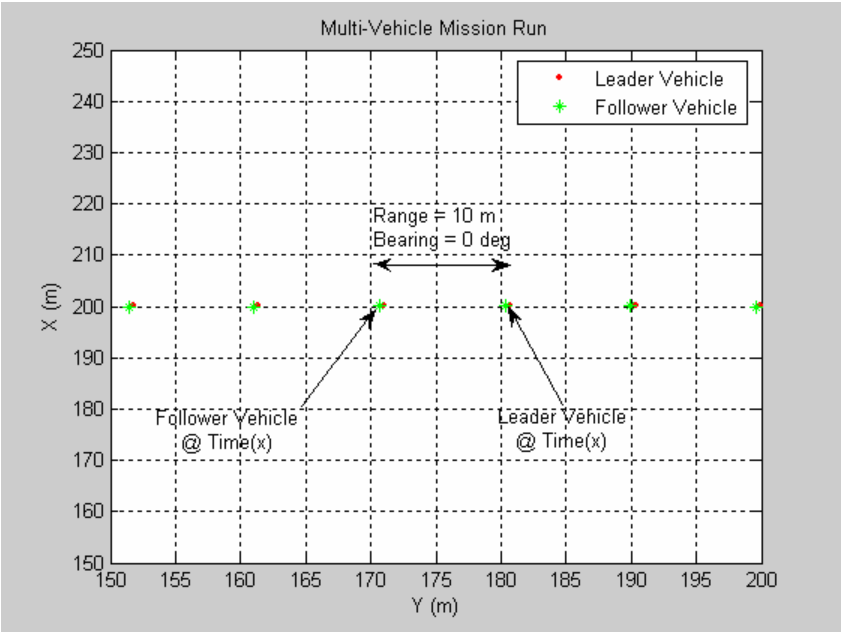

Figure 11. Zoomed In Look (Straight Path)

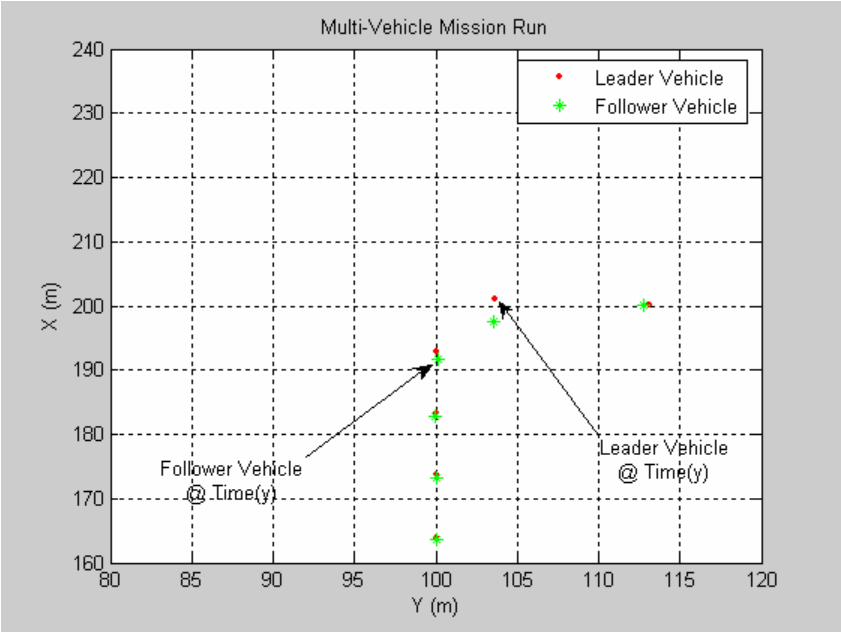

Figure 12. Zoomed In Look (Turn)

E. MULTIPLE VEHICLE SIMULATION (WITH CURRENT)

The next step of this thesis was to add the affects of current in to the simulation. Current was added to achieve a more accurate simulation of a real world mission. Figure 13 depicts the tracks for the leader and follower vehicles during the mission simulation containing the affects of current. Looking at Figure 9, the follower vehicle does not appear to be directly behind the leader vehicle as seen in the earlier simulation.

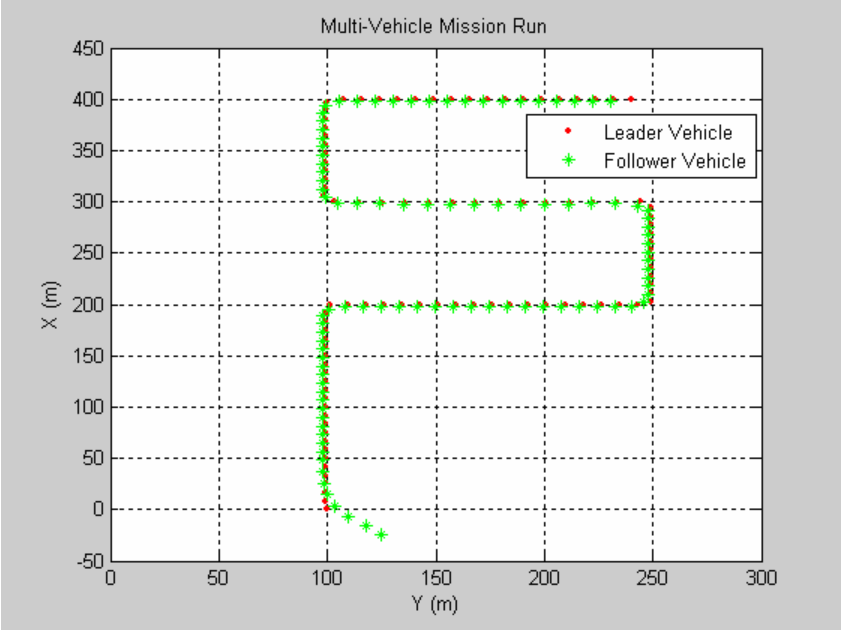

Figure 13. Leader and Follower Vehicle Path (affected by currents)

Figures 14 and 15 contain a "zoomed in" look at the mission simulation. Specifically, Figure 14 is a "zoomed in" look at the vehicles while they are traveling in a straight line. Figure 15 is a "zoomed in" look at the vehicles during a turn.

From Figure 13, it initially looks like the follower vehicle is offset in comparison to the leader vehicle. However, the leader vehicle actually has a range of 10 meters and a bearing of 0 degrees. This is shown in Figures 16 and 17. Both the leader and follower vehicles are "crabbed" in order to offset the current and reach the desired waypoints.

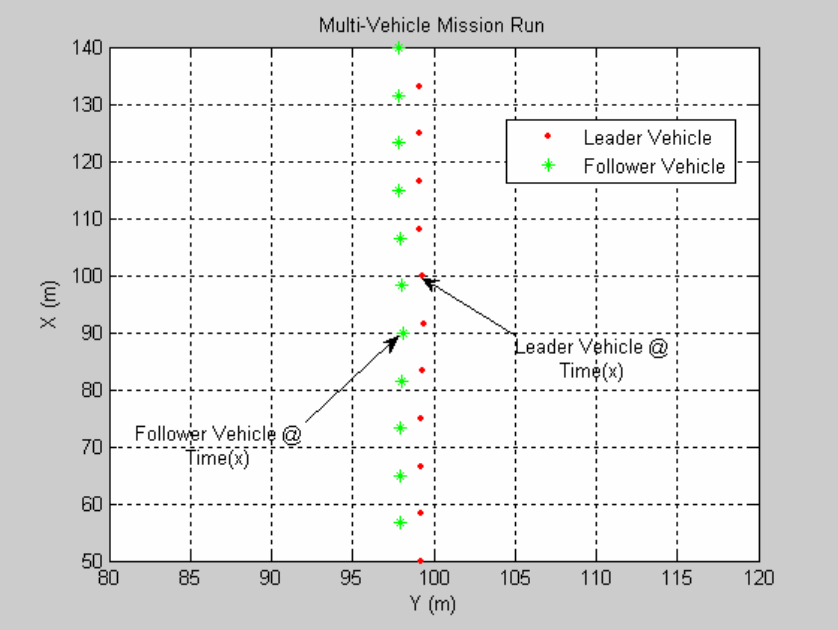

Figure 14. Zoomed In Look (Straight Path w/ Currents)

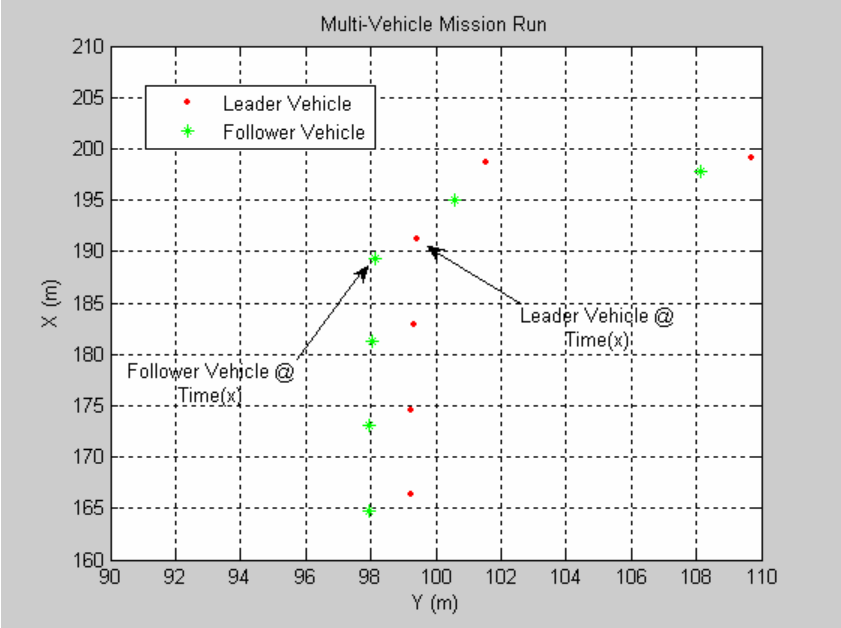

Figure 15. Zoomed In Look (Turn w/ Currents)

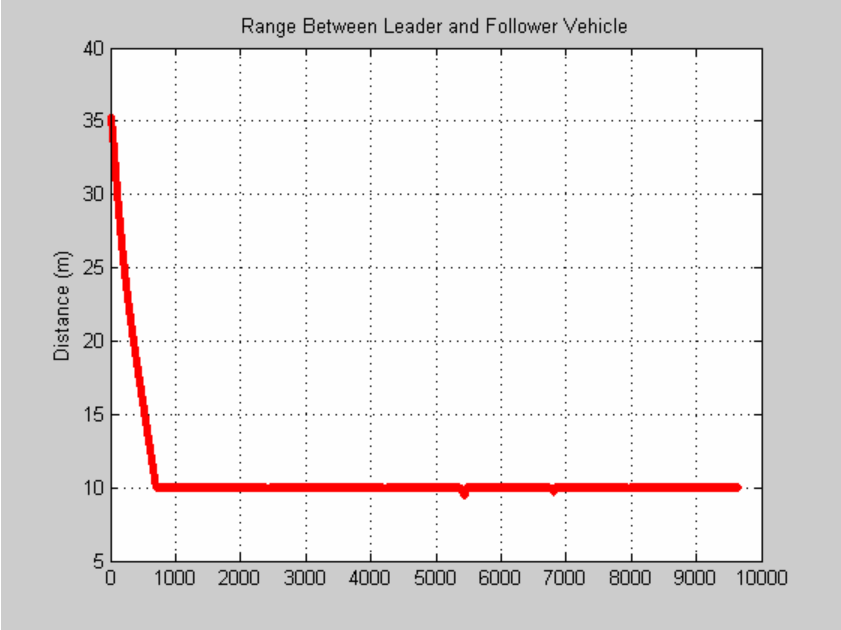

Figure 16. Range Between Leader and Follower Vehicle (w/ currents)

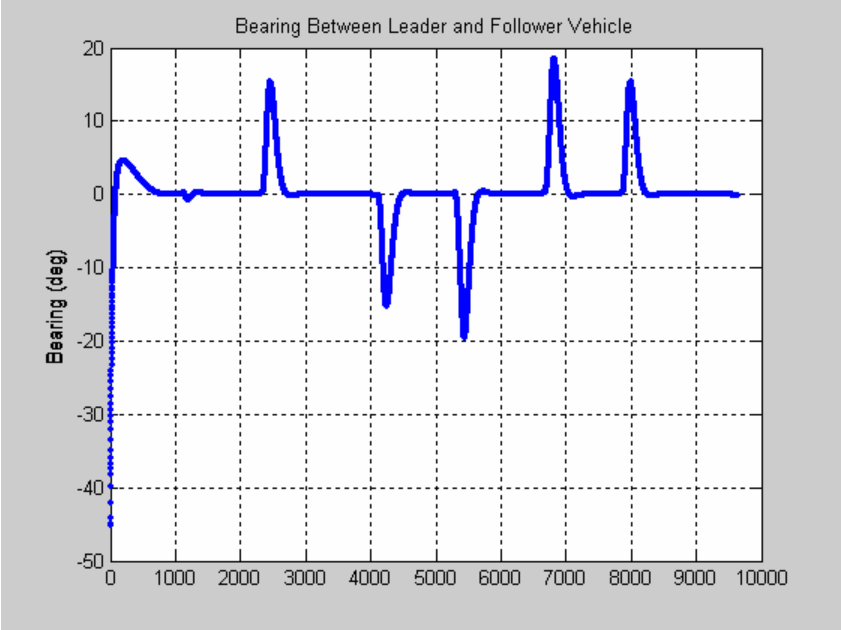

Figure 17. Bearing Between Leader and Follower Vehicle (w/ currents)

VI. CONCLUSIONS AND RECOMMENDATIONS

A. CONCLUSIONS

This thesis modeled and simulated formation flying of multiple AUV's using forward looking sonar as a method of controlling the position of the follower vehicle in the formation. The research completed by this thesis provides the tools necessary to develop more sophisticated cooperative behaviors (i.e., multiple vehicle obstacle avoidance). The proposed control laws presented in this thesis successfully operates in the simulation environment. The follower vehicle adjusted its speed and heading accordingly to obtain the commanded position accurately.

B. RECOMMENDATIONS

There are many areas in which this thesis work can be improved upon to build a more complete and robust formation model for the REMUS vehicle. One such area is the development of a three dimensional model. This would require the addition of depth to the sonar scan. This in turn would require the modification of the vehicle equations of motion to include diving and climbing maneuvers.

Another area of future work is to implement obstacle avoidance algorithms into the simulation. Obstacle avoidance algorithms have been designed for use with REMUS vehicles using forward looking sonar. However, it has yet to be expanded to multiple vehicle formations.

Lastly, upon completion of simulation modeling, real world experimentation must take place in order to validate results received form various simulations using forward looking sonar. After initial experimental data has been collected, the simulation model may need to be refined to account for environmental factors not originally foreseen by the model.

THIS PAGE INTENTIONALLY LEFT BLANK

APPENDIX

```
% Multi - Vehicle (Dependent Control)

% This m-file simulates a multi-vehicle follow the leader formation.
% It uses corrected hydrodynamic coeff from MIT to develop a steering
% model for the leader vehicle.  The follower vehicle is positioned
% based on bearing and range to the leader vehicle received from a
% forward looking sonar that is attached to the follower vehicle.

clear,close all;
clc

DegRad = pi/180;
RadDeg = 180/pi;

% REMUS Characteristic Specifications
L = 1.33;           % Length in m
W = 2.99e02;        % Weight in N
g = 9.81;           % Acceleration of gravity in m/s^2
m = W/g;            % Mass in kg
V = 1.543;          % Max Speed in m/s
rho = 1.03e03;      % Density of Salt H20 in kg/m^3
D = .191;           % Max diameter in m

% State Model Parameters
Uo  = 1.543;                    % in m/s
Boy = 2.99e02;
xg  = 0; yg = 0; zg = 1.96e-02; % in m

Iy = 3.45;                      % kg/m^3 (from MIT thesis)
Iz=Iy;

% MIT REMUS Coeff (Dimensionalized)
Nvdot = 1.93;
Nrdot = -4.88;
Yvdot = -3.55e01;
Yrdot = 1.93;
% Nv = -4.47; should be same as Mw which is stated as +30.7
% should be -9.3 but going by Hoerner eqn, we get about 4.47
Nv = -4.47;
Nr = -6.87;         % Same as Mq;
Yv = -6.66e01;
% Same as Zw; Note should be -6.66e1 from MIT thesis not 2.86e01
Yr = 2.2 ;          % Same as Zq = 2.2; MIT has miscalculation
Nd = -3.46e01/3.5;  % Nd and Yd scaled by 3.5 to align w/exp data
Yd = 5.06e01/3.5;

% REMUS Steering Equations
MM=[(m-Yvdot) -Yrdot 0;-Nvdot (Iz-Nrdot) 0;0 0 1];
AA=[Yv (Yr-m*V) 0;Nv Nr 0; 0 1 0];
BB=[Yd;Nd;0];
A=inv(MM)*AA; B=inv(MM)*BB; C=[0,0,1]; D=0;
```

```
A2=[A(1:2,1),A(1:2,2)];B2=[B(1);B(2)];
xss=inv(A2)*B2;
poles = eig(A2);
RadGy = sqrt(Iz/(W/g));                    % in m
RadCurv = Uo/(xss(1));                     % in m
SideSlip = atan2(xss(1),Uo)*180/pi;        % in deg/s

[num,den]=ss2tf(A,B,C,D); z=roots(num); p=roots(den);

% Desired closed loop poles for sliding
k=place(A,B,[-1.4,-1.45,0.0]);

% Closed loop dynamics matrix
Ac=A-B*k;
[m,n]=eig(Ac');
S=m(:,3);

%Define Sonar Grid Parameters:
%sonrange = 110;                  % radial range in m based on FLS chart
%theta = 2*pi/3;                  % angular arc in rad
%dtheta = 1*pi/180;               % angular bin length in rad
%thetab = theta/dtheta;           % number of bins angularly
%offset = 0;

% Set time of run
dt = 0.125/2;
t = [0:dt:1800]';
size(t);

% Set initial conditions
start=10;
v(1)   = 0.0;
r(1)   = 0.0;
rRM(1) = r(1);
r_com = zeros(1,length(t)-1);

vf(1)   = 0.0;
rf(1)   = 0.0;
rRMf(1) = rf(1);
r_comf = zeros(1,length(t)-1);

% This is the initial heading of the vehicle
psi(1) = 0.0*DegRad;

psif(1) = 0.0*DegRad;

% This is the initial position of the vehicle
X(1) = 0.0; % in m
Y(1) = 100.0;

Xf(1) = -25.0; % in m
Yf(1) = 125.0;
```

```
% This data from track.out file
No_tracks=7;
Track=[100.0 100.0 2.75 2.75  0  1.25  1.00 0 25.00 8.00 40.00
       200.0 100.0 2.75 2.75  0  1.25  1.00 0 25.00 8.00 200.00
       200.0 250.0 2.75 2.75  0  1.25  1.00 0 25.00 2.00 15.00
       300.0 250.0 2.75 2.75  0  1.25  1.00 0 25.00 2.00 200.00
       300.0 100.0 2.75 2.75  0  1.25  1.00 0 25.00 2.00 200.00
       400.0 100.0 2.75 2.75  0  1.25  1.00 0 25.00 2.00 200.00
       400.0 250.0 2.75 2.75  0  1.25  1.00 0 25.00 2.00 200.00];
track=Track(:,1:2);
SurfaceTime = Track(:,9);
SurfPhase   = Track(:,8);

% Read in waypoints from track data assumes track is loaded
for j=1:No_tracks,
   X_Way_c(j)     = track(j,1);
   Y_Way_c(j)     = track(j,2);
   end;

PrevX_Way_c(1) = X(1);
PrevY_Way_c(1) = Y(1);

% Set rudder angle saturation:
sat = 9; % Degrees

% Set Watch Radius:
W_R = 2.0;

% Set dead-reckoning/look-ahead distance:
rabbit = 7;

x(:,1) = [v(1);r(1);psi(1)];

xf(:,1) = [vf(1);rf(1);psif(1)];

Eta_FlightHeading = 0.5;    % Lowered this from 1.0 on ARIES model
Phi_FlightHeading = 0.1;    % Lowered this from 0.5 on ARIES model

% Below for tanh
Eta_CTE = 0.05;
Eta_CTE_Min = 1.0;
Phi_CTE = 0.2;

   Uc = 0.0;
   Vc = 0.0;

SegLen(1) = sqrt((X_Way_c(1)-PrevX_Way_c(1))^2+(Y_Way_c(1)-
PrevY_Way_c(1))^2);
psi_track(1) = atan2(Y_Way_c(1)-PrevY_Way_c(1),X_Way_c(1)-
PrevX_Way_c(1));
```

```
for j=2:No_tracks,
   SegLen(j) = sqrt((X_Way_c(j)-X_Way_c(j-1))^2+(Y_Way_c(j)-Y_Way_c(j-
1))^2);
   psi_track(j) = atan2(Y_Way_c(j)-Y_Way_c(j-1),X_Way_c(j)-X_Way_c(j-
1));
end;

  j=1;
  Sigma = [];
  Depth_com = [];
  dr=[];
  drl = [];
  drl(1) = 0.0;
  psint=[];

  Depth_com(1) = 5.0;
  WayPointVertDist_com = [5.0 5.0 5.0 5.0 5.0 5.0 5.0];

% Initialize path planning
start=zeros(1,length(t)-1);offset=start;
Xdev=start;Ydev=start;
count=0;
inplan=0;
psiapf=start;

% Begin mission simulation
for i=1:length(t)-1
Depth_com(i) = WayPointVertDist_com(j);

X_Way_Error(i) = X_Way_c(j) - X(i);
Y_Way_Error(i) = Y_Way_c(j) - Y(i);

% DeWrap psi to within +/- 2.0*pi;
 psi_cont(i) = psi(i);

   while(abs(psi_cont(i)) > 2.0*pi)
      psi_cont(i) = psi_cont(i) - sign(psi_cont(i))*2.0*pi;
   end;

% DeWrap psi_error to within +/- pi;
 psi_errorCTE(i) = psi_cont(i) - psi_track(j);

   while(abs(psi_errorCTE(i)) > pi)
      psi_errorCTE(i) = psi_errorCTE(i) - sign(psi_errorCTE(i))*2.0*pi;
   end;

% **Always calculate this**
Beta = 0.0;
cpsi_e = cos(psi_errorCTE(i)+Beta);
spsi_e = sin(psi_errorCTE(i)+Beta);
```

```
s(i) = [X_Way_Error(i),Y_Way_Error(i)]*...
       [(X_Way_c(j)-PrevX_Way_c(j)),(Y_Way_c(j)-PrevY_Way_c(j))]';

% s is distance to go projected to track line(goes from 0-100%L)
s(i) = s(i)/SegLen(j);

Ratio=(1.0-s(i)/SegLen(j))*100.0;

% ss is the radial distance to go to next WP
ss(i) = sqrt(X_Way_Error(i)^2 + Y_Way_Error(i)^2);

% dp is the angle between line of sight and current track line
dp(i) = ...
             atan2( (Y_Way_c(j)-PrevY_Way_c(j)),(X_Way_c(j)-
PrevX_Way_c(j)) )...
           - atan2( Y_Way_Error(i),X_Way_Error(i) );

      if(dp(i) > pi),
         dp(i) = dp(i) - 2.0*pi;
      end;

      cte(i) = s(i)*sin(dp(i));

      if( abs(psi_errorCTE(i)) >= 00.0*pi/180.0)

% Use LOS Control
         LOS(i) = 1;

         psi_comLOS(i) = atan2(Y_Way_Error(i),X_Way_Error(i));

         cc=0;
         psioalook(i)=0;
         r_com(i)=0.0;

        if cc>0
            psioatot(i)=psioalook(i)/cc;
        else
            psioatot(i)=psioalook(i);
        end;

% Integral control - limit error only activate if i>2
        psint(1)=0;
        ctel(i)=cte(i);

        if (abs(cte(i))> 2), ctel(i)=2*sign(cte(i));end;

        if (i>1),  psint(i)=psint(i-1)+dt*cte(i);end;

        psi_errorLOS(i) = psi_comLOS(i) - psi_cont(i)-
(atan2(cte(i),rabbit))*1.0 -0.0*psint(i)+
0.0*psioatot(i)+1.0*psiapf(i);
```

```
        if(abs(psi_errorLOS(i)) > pi),
           psi_errorLOS(i) = ...
           psi_errorLOS(i) -
2.0*pi*psi_errorLOS(i)/abs(psi_errorLOS(i));
        end;

        Sigma_FlightHeading(i) = (-S(1,1)*v(i))*0.0+S(2,1)*(r_com(i) -
r(i)) + S(3,1)*psi_errorLOS(i);

        % Have taken out v influence in Sigma_FlightHeading above

        dr(i) = (-k(1,1)*v(i))*0.0-k(1,2)*r(i) ...
                -
Eta_FlightHeading*tanh(Sigma_FlightHeading(i)/Phi_FlightHeading);
    else

% Use CTE Controller
      LOS(i) = 0;
      if(cpsi_e ~= 0.0), % Trap Div. by Zero !

% SMC Soln
      Sigma(i) = Uo*rRM(i)*cpsi_e + Lam1*Uo*spsi_e + Lam2*cte(i);

      dr(i) = (1.0/(Uo*a*cpsi_e))*(-Uo*b*rRM(i)*cpsi_e +
Uo*rRM(i)^2*spsi_e ...
            - Lam1*Uo*rRM(i)*cpsi_e - Lam2*Uo*spsi_e -
2.0*Eta_CTE*(Sigma(i)/Phi_CTE));

      else
         dr(i) = dr(i-1);
      end;

   end;% End of CTE Controller

   if(abs(dr(i)) > sat*pi/180) % change from 0.4 radians on ARIES
      dr(i) = sat*pi/180*sign(dr(i));end;

%Range and Bearing
Rcom  = 10;     %in m

range(i)=sqrt((Y(i)-Yf(i))^2+(X(i)-Xf(i))^2);

R_err(i)=range(i)-Rcom;

U(i)=(-sign(R_err(i))*range(i)+Uo*cos(psi(i))*(Xf(i)-
X(i))+Uo*sin(psi(i))*(Yf(i)-Y(i)))/(cos(psi(i))*(Xf(i)-
X(i))+sin(psi(i))*(Yf(i)-Y(i)));

Bcom = 0;

bearing(i)=atan2((Y(i)-Yf(i)),(X(i)-Xf(i)))-psif(i);
```

```
B_err(i)=bearing(i)-Bcom;


if (abs(B_err(i))>pi), B_err(i)=B_err(i)-2*pi*sign(B_err(i));end;


drf(i)=-5*B_err(i)+10*rf(i);
maxspeed = 2;
minspeed = 1;

if U(i)<minspeed
    U(i)=minspeed;
end;

if U(i)>maxspeed
    U(i)=maxspeed;
end;

% State Variable Formulation
x_dot(:,i+1) = [ A(1,1)*v(i) + A(1,2)*r(i) + B(1)*dr(i);
                 A(2,1)*v(i) + A(2,2)*r(i) + B(2)*dr(i);
                  r(i)];
x(:,i+1) = x(:,i)+dt*x_dot(:,i);
v(i+1)   = x(1,i+1);
r(i+1)   = x(2,i+1);
psi(i+1) = x(3,i+1);
rRM(i+1) = r(i+1);

x_dotf(:,i+1) = [ A(1,1)*vf(i) + A(1,2)*rf(i) + B(1)*drf(i);
                  A(2,1)*vf(i) + A(2,2)*rf(i) + B(2)*drf(i);
                  rf(i)];
xf(:,i+1) = xf(:,i)+dt*x_dotf(:,i);
vf(i+1)   = xf(1,i+1);
rf(i+1)   = xf(2,i+1);
psif(i+1) = xf(3,i+1);
rRMf(i+1) = rf(i+1);

% Kinematics
X(i+1) = X(i) + (Uc + (Uo)*cos(psi(i)) - v(i)*sin(psi(i)) )*dt;
Y(i+1) = Y(i) + (Vc + (Uo)*sin(psi(i)) + v(i)*cos(psi(i)) )*dt;

Xf(i+1) = Xf(i) + (Uc + (U(i))*cos(psif(i)) - vf(i)*sin(psif(i)) )*dt;
Yf(i+1) = Yf(i) + (Vc + (U(i))*sin(psif(i)) + vf(i)*cos(psif(i)) )*dt;

%  Check to see if we are within the WR or if we passed the WP
%  Change to next WP if radial distance to go is less than rabbit
%  distance or if we passed the WP or if we are within the WR

   if(sqrt(X_Way_Error(i)^2.0 + Y_Way_Error(i)^2.0) <= W_R | s(i) <
0.0| ss(i)<rabbit )
   disp(sprintf('WayPoint %d Reached',j));
      if(j==No_tracks),
%          PLOT_PART = 1;
```

```
            break;
        end;
        PrevX_Way_c(j+1) = X_Way_c(j);
        PrevY_Way_c(j+1) = Y_Way_c(j);
        j=j+1;
    end;

 end;

dr(i+1) = dr(i);
cte(i+1) = cte(i);
s(i+1) = s(i);
ss(i+1) = ss(i);
range(i+1)=range(i);
bearing(i+1)=bearing(i);
R_err(i+1)=R_err(i);
U(i+1)=U(i);

figure(1);
 for i=1:100:length(Y)
 plot(Y(i),X(i),'r.'); title('Multi-Vehicle Mission Run'); xlabel('Y
(m)'), ylabel('X (m)'); legend('Leader Vehicle','Follower Vehicle');
 axis([0 300 -50 450]);
 hold on
 plot(Yf(i),Xf(i),'g*');
 axis([0 300 -50 450]);
 grid on; hold on,
end;

figure(2);
plot(range,'r.'); title('Range Between Leader and Follower Vehicle');
ylabel('Distance (m)');
grid on;

figure(3);
plot(bearing.*180/pi,'b.'); title('Bearing Between Leader and Follower
Vehicle'); ylabel('Bearing (deg)');
grid on;
```

LIST OF REFERENCES

Blidberg, Richard D., "The Development of Autonomous Underwater Vehicles (AUVs); A Brief Summary", Autonomous Undersea Systems Institute, ICRA, Seoul, Korea, May 2001.

Clark, Vernon, "Seapower 21, Projecting Decisive Force Capabilities", United States Naval Institute Proceedings, October 2002, www.usni.org .

Department of the Navy (2004). *The Navy Unmanned Undersea Vehicle (UUV) Master Plan.* Retrieved April 11, 2005 from www.chinfo.**navy**.mil/navpalib/technology/**uuv**mp.pdf.

Fodrea, Lynn, "Obstacle Avoidance Control for the REMUS Autonomous Underwater Vehicle", Naval Postgraduate School, December 2002.

Healey, Anthony J., Marco, D. B., "Slow Speed Flight Control of Autonomous Underwater Vehicles: Experimental Results with NPS AUV II" *Proceedings of the 2nd International Offshore and Polar Engineering Conference, San Francisco*, July 14-19 1992.

Healey, Anthony J., *Dynamics of Marine Vehicles (MA-4823),* Class Notes, Naval Postgraduate School, Monterey, CA, 1995.

Healey, Anthony J., "Command and Control Demonstrations with Cooperating Vehicles", ONR Research Proposal in response to ONR BAA 01-012 "Demonstration of Undersea Autonomous Operation Capabilities and Related Technology Development", August 2001.

Hoerner, Sighard. Fluid Dynamic Drag. Published by author, 1965.

Johnson, Jay, "Parameter Identification of the ARIES AUV," M.S. Thesis Naval Postgraduate School, Monterey, CA, June 2001.

Kucik, Daniel, "Follow the leader Tracking by Autonomous Underwater Vehicles Using Acoustic Communications and Ranging," Naval Postgraduate School, September 2003.

Leonard, Naomi E., Fiorelli, Edward, Bhatta, Pradeep, Paley, Derek, "Multi-AUV Control and Adaptive Sampling in Monterey Bay," Proc. IEEE Autonomous Underwater Vehicles 2004: Workshop on Multiple AUV Operations, June 2004.

Marco, D.B and A.J. Healey, “Command, Control and Navigation Experimental Results With the NPS ARIES AUV,” IEEE Journal of Oceanic Engineering – Special Issue, 2001.

Miller, Timothy F., Walter, Jeremy L., Kiely, Daniel H., “A Next-Generation AUV Energy System Based on Aluminum-Seawater Combustion”, Presented June 2002 at AUV 2002: A Workshop on AUV Energy Systems, IEEE.

Prestero, Timothy, “Verification of a Six-Degree of Freedom Simulation Model for the REMUS Autonomous Underwater Vehicle,” M.S. Thesis Massachusetts Institute of Technology, Sep 2001.

INITIAL DISTRIBUTION LIST

1. Defense Technical Information Center
   Ft. Belvoir, Virginia

2. Dudley Knox Library
   Naval Postgraduate School
   Monterey, California

3. Mechanical Engineering Department Chairman, Code ME
   Naval Postgraduate School
   Monterey, California

4. Mechanical Engineering Curriculum, Code 34
   Naval Postgraduate School
   Monterey, California

5. Professor Anthony J. Healey, Code ME/HY
   Department of Mechanical Engineering
   Naval Postgraduate School
   Monterey, California

6. Doug Horner
   Naval Postgraduate School
   Monterey, California

7. LT Jason Grabelle
   Norfolk Naval Shipyard
   Norfolk, Virginia